Henryk BĄKOWSKI*

COMPUTER AIDED ANALYSIS OF WEAR OF THE SURFACE LAYER WITH A PEARLITIC STRUCTURE USING AN AMSLER STAND

KOMPUTEROWE WSPOMAGANIE ANALIZY ZUŻYCIA WARSTWY WIERZCHNIEJ O STRUKTURZE PERLITYCZNEJ NA STANOWISKU AMSLERA

Key words:

wear, surface layer, microstructure, pearlite, FEM, Amsler

Słowa kluczowe:

zużycie, warstwa wierzchnia, mikrostruktura, perlit, MES, Amsler

Abstract

The paper presents laboratory research results of the samples made of heat treated pearlitic rail steel. The tests were performed on an Amsler stand. The surface layer of metallographic specimens after sliding in various operational conditions is presented. The surface layer changed due to ratchetting where significant impact of various operational factors was observed. Simulation studies with the application of a finite element method (MES) followed. Each separate zone of the surface layer was reflected by the CAD system. Based on

* Silesian University of Technology, Faculty of Transport, ul. Krasińskiego 8, 40-019 Katowice, Poland, e-mail: henryk.bakowski@polsl.pl.

theoretical models, each individual zone was prescribed certain properties in order to specify the boundary conditions essential for numerical calculations to be performed. The obtained results made it possible to determine the zones particularly exposed to wear as well as the distribution of stress and deformation that enabled the determination of the depth of the retention of maximal values mentioned above.

INTRODUCTION

The observed wear processes of metal parts differ in specific features and mechanism of wear development. The images of the surface layer wear are also different in the following ways **[L. 1]**:

– Friction surface appearance,
– Structural changes in the material of the surface layer,
– The wear mechanism in the material of the surface layer, and
– The shape and size of wear products as well as their composition.

The reasons why products are withdrawn from the service can be diverse. However, the most frequently observed are abrasive and /or adhesive or fatigue wear subsequently followed by other types of wear **[L. 2]**. Wheel pressure causes the material upon the rolling surface to displace, i.e. 'flow', and the permanent deformations lead to the formation of flake wear products. Together with the increased number of cycles, the flakes formed can be the main cause of fatigue cracks. The process is known as ratchetting **[L. 3]**. Ratchetting is the process in which deformation is accumulated in the main dislocation direction of the load in the course of subsequent cycles **(Fig. 1)**. According to the dislocation theory of defects, clusters of dislocation function as localized stress, which appear when obstacles are met. The growth of stress generates new dislocations, which move when the yield point is exceeded. As the result of the mutual locking of moving dislocations and the presence of alloy elements as an admixture, gradual deformation strengthening is observed **[L. 4]**.

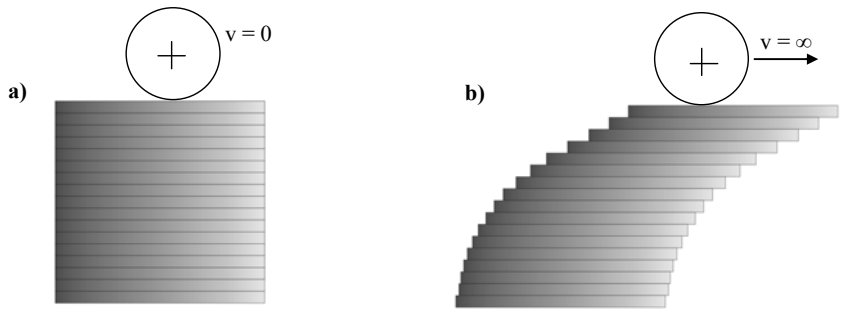

Fig. 1. Surface layer of the rail: a) before operation, b) after operation [L. 3]
Rys. 1. Schemat warstwy powierzchniowej szyny: a) przed eksploatacją, b) po eksploatacji **[L. 3]**

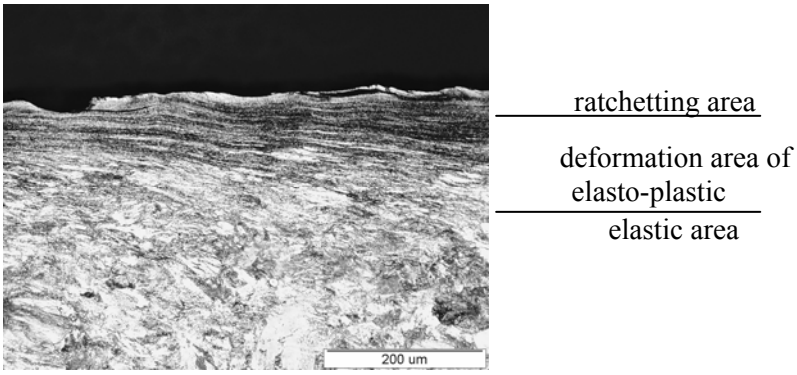

Fig. 2. Cross section of surface layer of a rail after operation
Rys. 2. Przekrój poprzeczny warstwy powierzchniowej szyny po eksploatacji

Strengthening of rail material after a longer period of track operation causes its degradation and contributes to the formation of fatigue cracks in the rail. Simultaneously, due to the formation of shear stresses, plastic 'flow of material' appears **[L. 4]**. The material 'flows' along the rail under the direction of the rolling wheel and in the transverse direction, towards the rolling edge of the rail **(Fig. 2)**. The reaction of the material in a contact zone wheel/rail is a four-step process as shown in **Figure 3**.

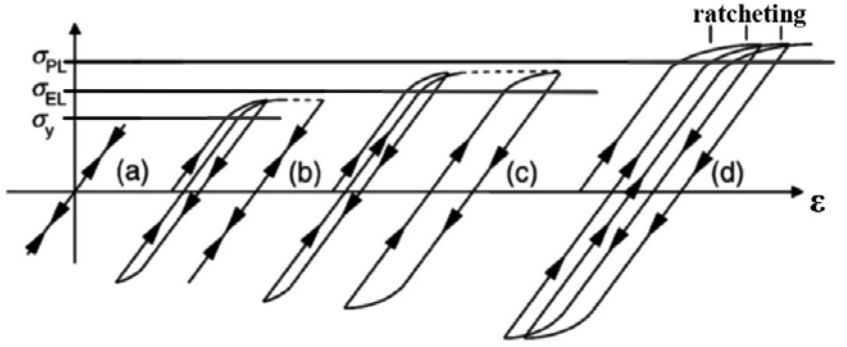

Fig. 3. Mechanism of ratchetting formation in system б-ε: бy – limit of proportionality, $б_{EL}$ – elastic limit, $б_{PL}$ – yield point [L. 3]
Rys. 3. Mechanizm tworzenia zjawiska ratchettingu w układzie б-ε: бy – granica proporcjonalności, $б_{EL}$ – granica sprężystości, $б_{PL}$ – granica plastyczności **[L. 3]**

As the result of multiple interaction of variable operational factors, the process of deformation accumulating in the surface layer (ratchetting) runs in four steps. In the first step, (a) deformations do not exceed the limit of proportionality, thus all changes taking place both on the rolling surface and under it are fully reversible. In the second step, (b) deformations show both the

resilient and resilient-plastic nature. The curve σ-ε is of a linear nature in accordance with the Hooke's Law and has the form of a loop typical for stresses that generate deformations.

In the third step, (c) together with the growth of pressure, the material starts to strengthen which leads to plastic deformations. The initial state lasts through several cycles before the curve of deformation stress forms a hysteresis loop and is transformed into a stationary stress curve that strains the system state. After the yield point is exceeded, the phenomenon of ratchetting occurs. Plastic deformation, being the reaction of the material, might be the cause of contact-fatigue deformations **[L. 3–5]**.

CHARACTERISTIC OF ROLLING-SLIDING CONTACT WITH PEARLITIC STRUCTURE

While the wheels roll on a rail, both the wheel and the rail undergo deformation and the point of contact changes into a contact zone. The contact zone is elliptical for the ideally profiled surface of the wheel and the railhead. When the wheel runs over the rail, adhesion or sliding appears in various parts of the area. These forces spread over the contact area appear as tangential stress, whereas the distribution of shear stresses depends on shape and size of this area, sliding values, and the state of running surfaces.

The point of the contact of a wheel running over a rail is small, ranging between 100–150 mm^2 and is determined by the profile and the wear degree of both the wheel and rail running surface. The shape of the contact surface and pressure distribution in the wheel-rail system as well as the roller-roller system is presented in **Fig. 4**. Distribution of surface stresses over the contact zone is an ellipse or a cylinder **(Figs. 4a, b)** described by the following equation **[L. 6]**:

$$p(x,y) = \frac{3 \cdot P}{2 \cdot \pi \cdot a \cdot b} \cdot \sqrt{1 - \left(\frac{x}{a}\right)^2 - \left(\frac{y}{b}\right)^2} \tag{1}$$

The relation described by the equation **[L. 7]** occurs between hardness and the module of longitudinal elasticity (Young's modulus):

$$HV = 0.0608 \bullet E \tag{2}$$

Figure 4 shows the stress distribution upon the contact surface according to (1) as well as pressure values in the roller-roller system.

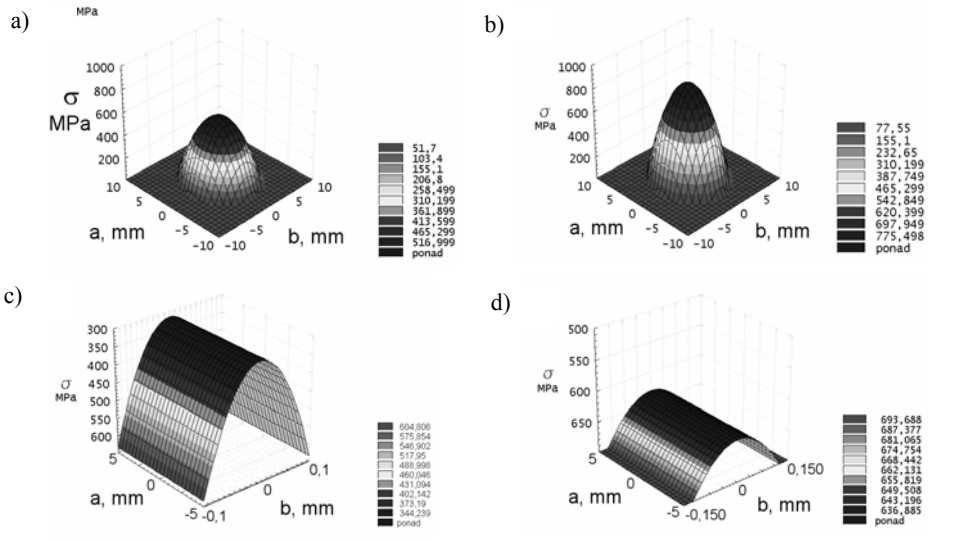

Fig. 4. Stress distribution in the wheel-rail system under the load: a) P = 100 kN, b) P = 150 kN and the roller-roller: c) P = 1000 N, d) P = 2000 N

Rys. 4. Rozkład nacisków w układzie koło-szyna przy obciążeniu: a) P = 100 kN, b) P = 150 kN i rolka-rolka: c) P = 1000 N, d) P = 2000 N

The analysis of wheels slippage over the rails in an established motion in which wheels of the set of rail vehicles roll in circles with unchangeable radius routed through their points of contact with rails prove that we deal here with a straight track where side swaying occurs. In the case of motion statically transient, which is observed in a curve, continuous but periodical variation of the radius of rolling circle of both wheels in each set of rail vehicles occurs. Areas of slippages and adhesion are presented in **Fig. 5**.

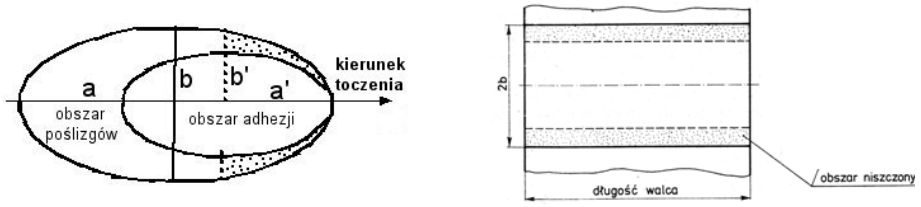

Fig. 5. Contact area in wheel-rail and roller-roller pairing (the ratio of the axle shaft a/b = a'/b') [L. 6].

Rys. 5. Obszar styku w skojarzeniach koło-szyna oraz rolka-rolka (stosunek półosi a/b = a'/b') **[L. 6]**

Adhesion and tearing off of the surface irregularities of the sliding elements takes place in the area of adhesion. A White Etching Layer (WEL),

which is formed during operation, can be observed in the surface layer of elements working in a rolling-sliding contact. WEL then generates cracks and chippings.

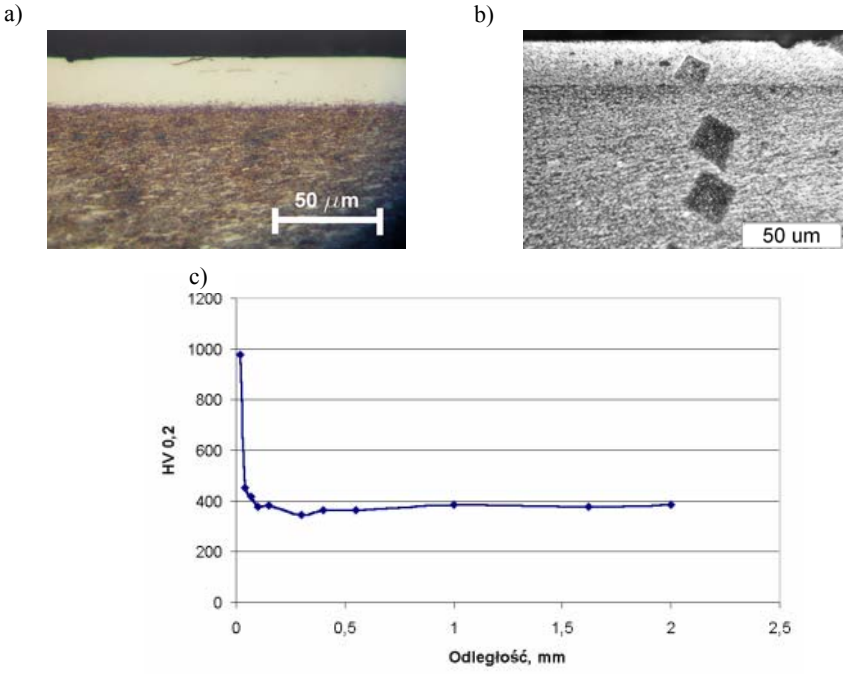

Fig. 6. Surface layer (a, b) and hardness spread (c) of a rail after operation.
Rys. 6. Warstwa powierzchniowa (a, b) i rozkład twardości (c) szyny kolejowej po współpracy

In the contact zone of the wheel-rail at a certain depth under the contact surface at the "Bielajew point," the most profound tangential stresses occur. They move towards the surface as the friction forces, which affect the contact zone together with normal stress, increase. This might be the reason for the initiation of microcracks that turn into macrocracks **(Fig. 7)**. The final effect is tearing off the pieces of material from the surface layer of the rolling surface **[L. 7]**.

The issue of WEL formation is interesting, because thorough knowledge about it might help prolong the life of rails **[L. 8]**. The surface layer is 10–100 μm thick, white in colour after etching with nital (a), and iron chloride (b) **(Figure 6)** can be observed under an optic microscope on metallographic specimens in the wheel and rail cross-section.

The first step in defect formation is when WEL, with the length of approximately 1 mm, a width of 0.1 mm, and a depth of around 10 μm, appears upon the rail surface. During further operation, spots grow and form the dotted layer. Since the white layer features greater hardness than pearlitic steel (the rails

are made of pearlitic steel), the speed of layer destruction decreases. On the other hand, when the thickness of WEL exceeds the cracks, chipping takes place.

Table 1. Values of material constants used in MES computations
Tab. 1. Wartości stałych materiałowych użytych w obliczeniach MES

Feature Material	Young's modulus E, GPa	Poisson's ratio v	Tensile strength R_m, MPa
Ferrite	180–210	0.25	350–590
Cementite	260–282	0.29	–5000

Calculations of stress distributions and deformations were performed with the application of a Femap and Nastran solver. The values of material constants were assumed based on literature **[L. 9]**, and their extreme values are listed in **Table 1**. Plates of cementite (0.05 μm) and ferrite (0.5 μm) **[L. 10]** of a simplified shape **(Figure 8)** were taken for computations.

RESULTS

The studies of the microhardness of the surface layer made it possible to determine its value and the impact of the selected operational parameters upon the depth and direction of plastic deformations **(Fig. 7)**.

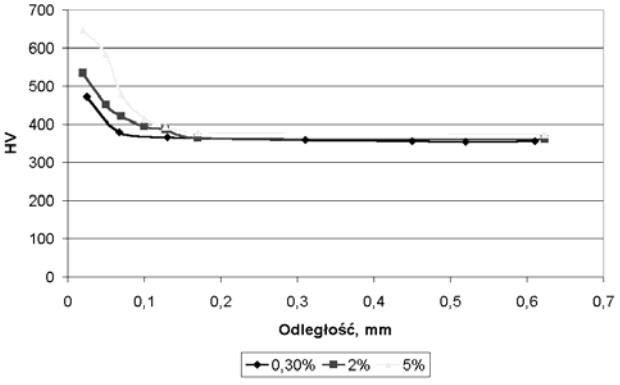

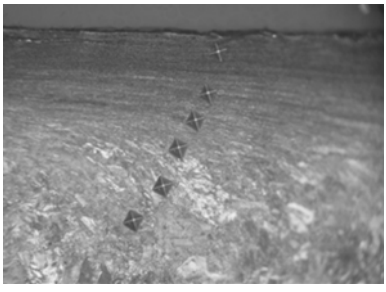

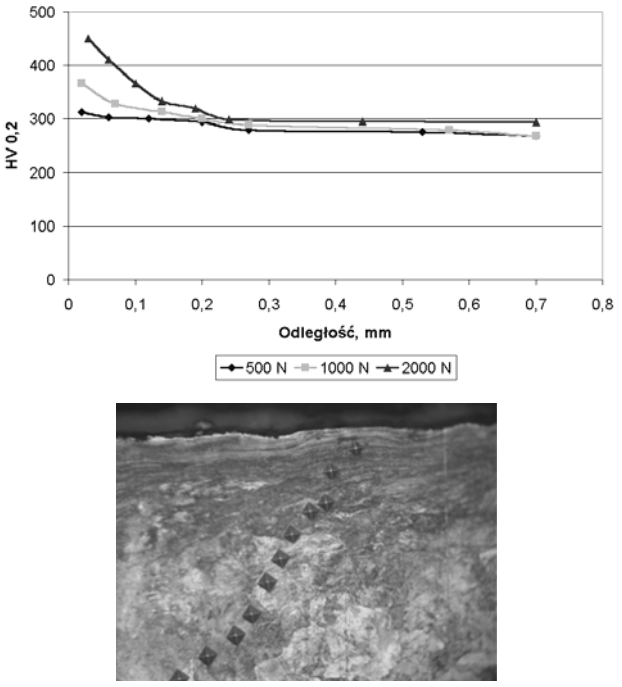

Fig. 7. Changes in microhardness as a function of distance from the samples surface made of R260 steel in relation to changing operational parameters, mag. ×200

Rys. 7. Zmiany mikrotwardości w funkcji odległości od powierzchni próbek ze stali R260 w zależności od zmiennych parametrów eksploatacji, pow. ×200

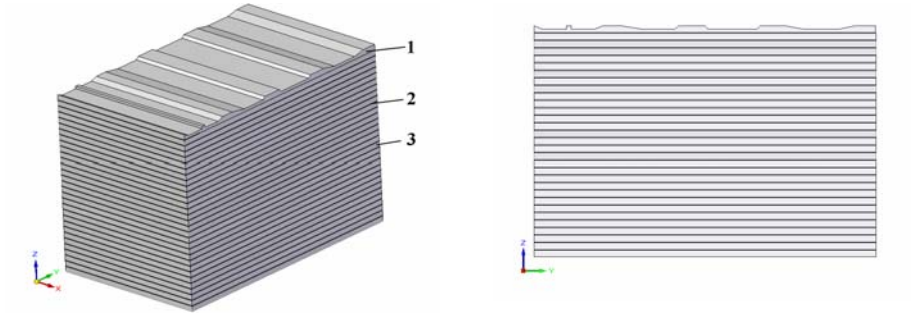

Fig. 8. Geometrical model of the surface layer with pearlitic structure: 1 – simplified real contact surface, 2 – layer of cementite, 3 – layer of ferrite

Rys. 8. Model geometryczny warstwy wierzchni o strukturze perlitycznej: 1 – uproszczona rzeczywista powierzchnia kontaktu, 2 – warstwa cementytu, 3 – warstwa ferrytu

The results of numerical computations of stress and the deformation distribution of the studied pairing are presented in **Figures 9, 10 and 11**. The results show that the values of local stresses in cementite plates in the close vicinity of the sliding surface amount to 300 MPa **(Fig. 9)**. Ferrite plates, due to

much worse resistance properties, undergo deformation which may lead to the local phenomenon of decohesion **(Fig. 11)**.

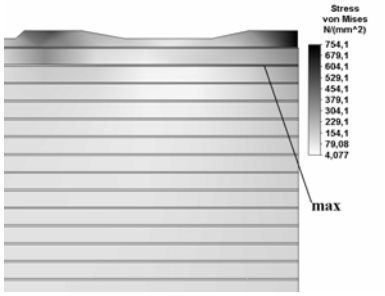

Fig. 9. Stress distribution in the surface layer in pearlite grain micro-scale
Rys. 9. Rozkład naprężeń w warstwie wierzchniej w mikroskali ziarna perlitu

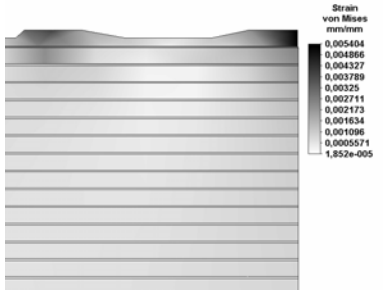

Fig. 10. Deformation distribution in the surface layer in pearlite grain micro-scale
Rys. 10. Rozkład odkształceń w warstwie wierzchniej w mikroskali ziarna perlitu

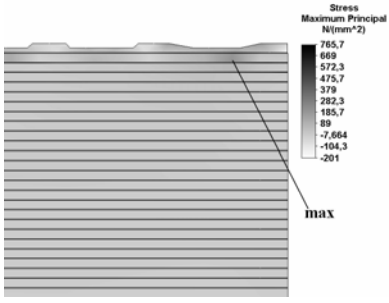

Fig. 11. Tensile stress distribution in the surface layer in pearlite grain micro-scale
Rys. 11. Rozkład naprężeń rozciągających w warstwie wierzchniej w mikroskali ziarna perlitu

CONCLUSIONS

The studies used rolling-sliding pairing that reflected the conditions of a wheel-rail system. The material used for investigations was a pearlitic structure with ferrite and cementite plates arranged in alternating order. Quantitative metallographic analysis was performed in order to define the thickness of ferrite

and cementite plates. Based on the analysis, the model of pearlite structure was developed and numerical computations were performed. Additionally, a simplified model of a real contact surface was built.

The thickness of thin cementite plates as well as the shape of a real surface affect the value and stress distribution in the pairing. It is because von Mises major reduced stresses reside in these zones. It should be expected that the morphology of plates Fe_3C have a decisive impact upon the strength and inclination to cracking of the material. On the basis of a 3D model of a detailed pearlitic structure as well as the determination of material constants, it was possible to state that, in order to determine zones prone to cracking, it is necessary to carry out both (MES) and metallographic simulation studies.

REFERENCES

1. Massel A.: Faliste zużycie szyn a warunki eksploatacyjne. Problemy Kolejnictwa, CNTK z.127, Warszawa 1998, 76–98.
2. Kristan J., Sawley K.: Material property characterization and specifications for improved rail steel. TTCI R&D, Railway Track and Structures, October 2002, 14–16.
3. Su X., Clayton P.: Ratchetting strain experiments with a pearlitic steel under rolling/sliding contact. Wear 205 1997, 137–143.
4. Bon-Woong Koo at all: Experimental measurement of Young's modulus from a single crystalline cementite. Scripta Materialia 82, 2014, 25–28.
5. Zubkova T.A., Yakovleva I.L., Karkina L.E., Veretennikova I.A.: Study of the hardness and elastic modulus of cementite in the structure of granular pearlite by the nano-indentation method. Metal Science and Heat Treatment, Vol. 56, 2014, 5–6.
6. Böhmer A. i inni: Beanspruchungen von schienen unter statischen, dynamischen und thermishen belastungen. Glasers Annalen 127 3,4/2003, 116–130.
7. Pytko S.: Problemy wytrzymałości kontaktowej. PAN Warszawa 1982.
8. Pointner P.: Auswirkungen des Rad-Schiene-Kontaktes auf Werkstoffwahl und Fahrweggüte. Eisenbahningenieur (51), 9/2001, 122–126.
9. Muskalski Z., Milenin A.: Development of Finite Element Model of Reorientation of Cementite Lamellae in Pearlite Colonies in Wire Drawing Process for Wires Made from High Carbon Steel. Solid State Phenomena, Vol. 165 (2010) pp. 136–141.
10. Posmyk A., Bąkowski H.: Zużywanie w mikroskali skojarzenia żeliwny pierścień tłokowy-kompozytowa tuleja cylindrowa. Tribologia 3, 2015, 153–162.

Streszczenie

W pracy przedstawiono wyniki badań laboratoryjnych na stanowisku Amslera próbek wykonanych ze stali szynowej bez obróbki cieplnej o strukturze perlitycznej. Zaprezentowano warstwę wierzchnią zgładów metalograficznych po współpracy w różnych warunkach eksploatacji.

Warstwa wierzchnia uległa zmianie na skutek zjawiska ratchettingu poprzez oddziaływanie różnych czynników eksploatacyjnych. Następnie posłużono się badaniami symulacyjnymi ze pomocą metody elementów skończonych (MES). Odzwierciedlono poszczególne strefy warstwy wierzchniej za pomocą systemu CAD. W oparciu o modele teoretyczne nadano poszczególnym strefom właściwości, aby określić warunki brzegowe niezbędne do przeprowadzenia obliczeń numerycznych. Uzyskane wyniki pozwoliły na określenie miejsc szczególnie narażonych na zużycie oraz rozkłady naprężeń i odkształceń umożliwiające wyznaczenie głębokości zalegania maksymalnych ww. wartości.